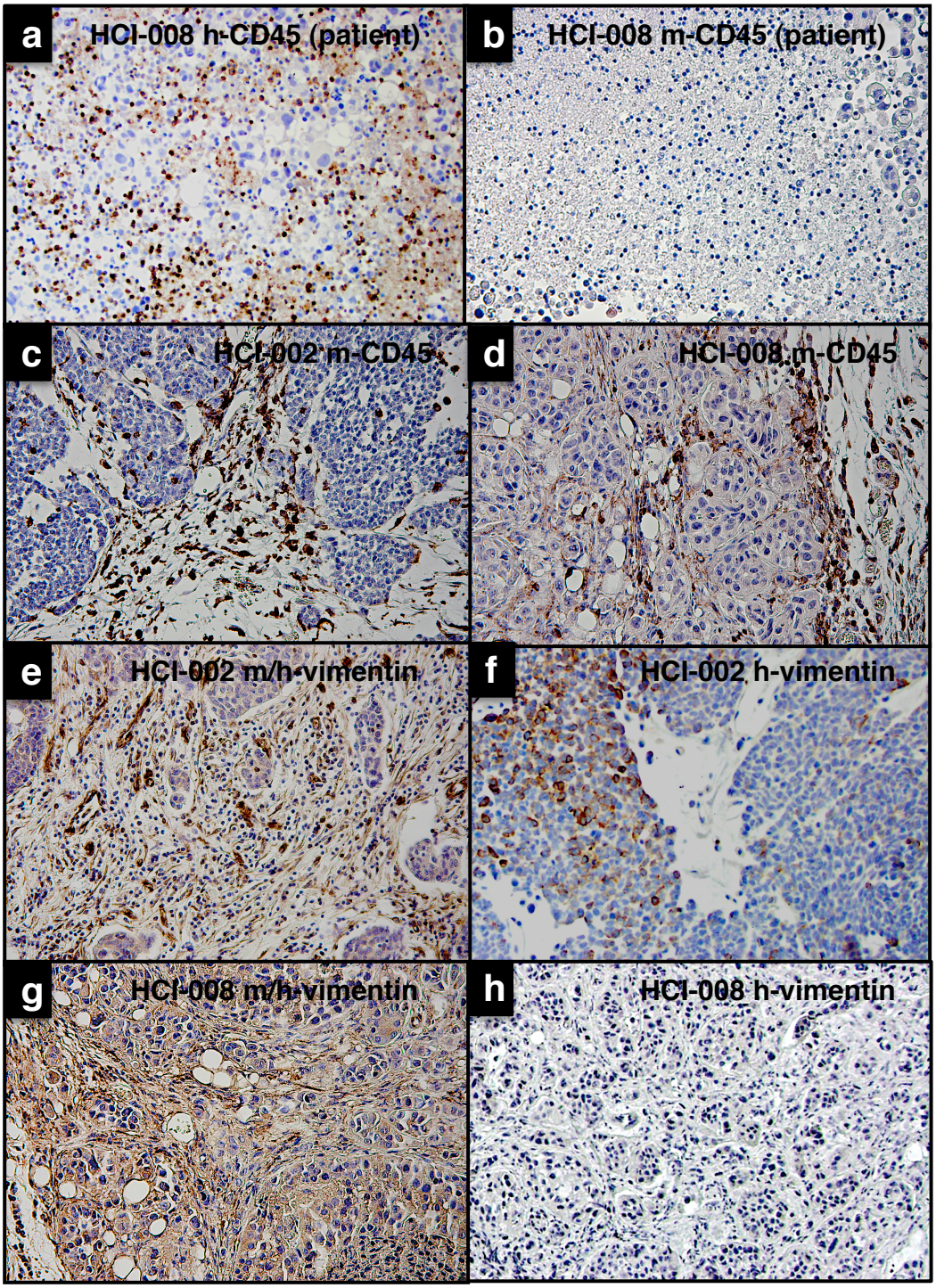

Supplementary Figure 15. Human tumor grafts are infiltrated with mouse-derived stroma. **a-d.** Representative images showing infiltration of murine leukocytes into tumor grafts. An antibody specific for human CD45 shows positive staining on the original patient specimen from which HCI-008 was derived (a), while no human-specific CD45 staining is observed in tumor grafts (also see Supplementary Figure 22 for HCI-008). On the other hand, an antibody specific for mouse CD45 does not react with human CD45+ cells on the original patient specimen (b), but does react with mouse-derived leukocytes. Representative pictures from two tumor grafts are shown: HCI-002 (c) and HCI-008 (d). **e-h.** Representative images showing recruitment of murine fibroblasts into human tumor grafts. Two tumor graft lines are shown, HCI-002 (e,f) and HCI-008 (g,h). Stromal cells in both lines stain positive with antibodies recognizing both mouse and human vimentin (e,g). On the other hand, antibodies specific for human vimentin react only with a few vimentin-positive tumor cells in HCI-002 (f) but not with stromal cells in either tumor graft line (f,h).

HCI-009	# mice from which organs sectioned			Patient information	
Generation	**lymph nodes**	**lung**	**bone**	metastasis	vital status
1º graft	3/3	3/3	0/1 (examined due to suspicious X-ray)	Lymphatics, bone, pancreas, peritoneum	Dead
2º graft	3/3	3/3			
3º graft	3/3	3/3			
total	**9/9**	**9/9 (micromets only)**			
frequency	**100%**	**100%**			
frequency of both LN and lung involvement		**100%**			

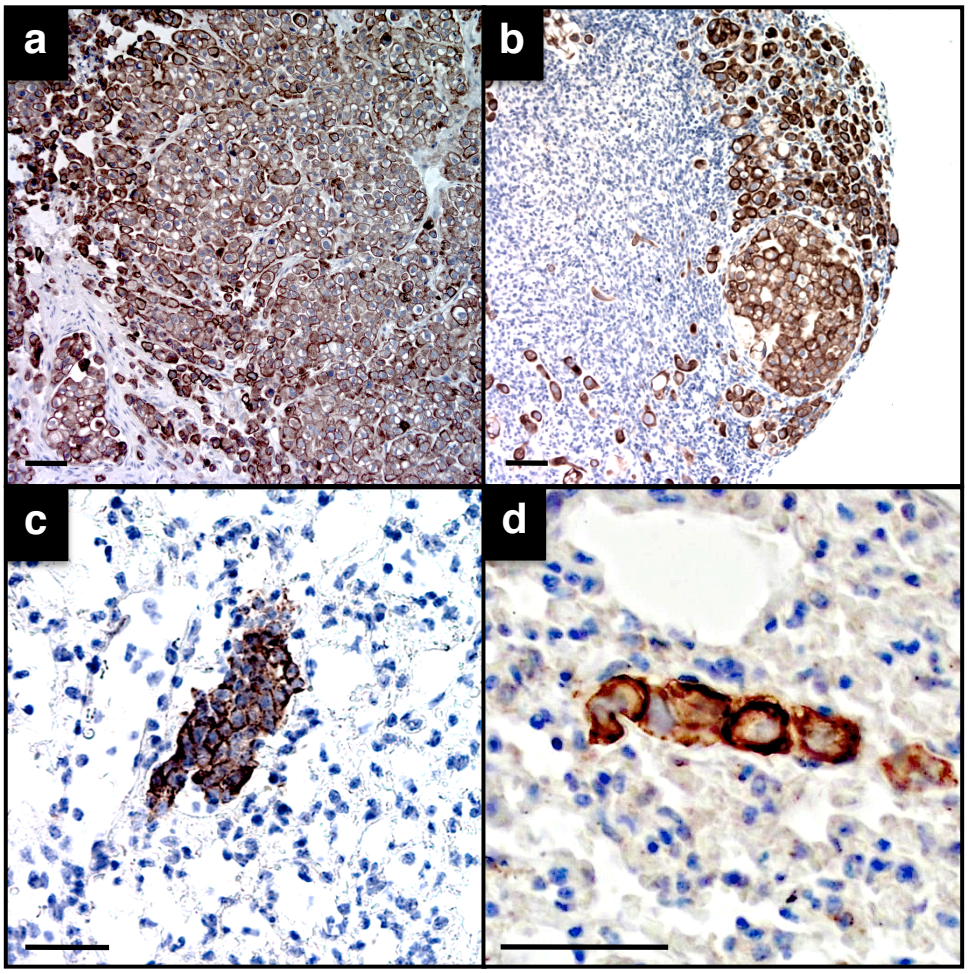

Supplementary Figure 16. Summary of metastasis from HCI-009. Top: Table illustrating the frequency of metastasis from three different tumors from three different generations of grafts, as well as clinical information on the patient from which HCI-009 was derived. Metastases were detected in lymph nodes and lungs of all mice examined, but bone metastasis was not evident in the single sample examined (only bones with suspicious X-rays were examined histologically). Bottom: Representative images illustrating the histological characteristics of HCI-009 tumor graft (a) and metastases in lymph node (b) or lung (c,d). All images in a-d show immunohistochemical staining for cytokeratin. Scale bars represent 100 microns.

HCI-005	# mice from which organs sectioned		Notes	Patient information	
Generation	**lymph nodes**	**lung**		metastasis	vital status
1º graft	2/4	3/4	mice also develop peritoneal metastasis	Lung, bone	Dead
2º graft	1/5	3/5			
3º graft	2/4	2/4			
total	**5/13**	**8/13**			
frequency	**38%**	**62%**			
frequency of both LN and lung involvement		**31%**			

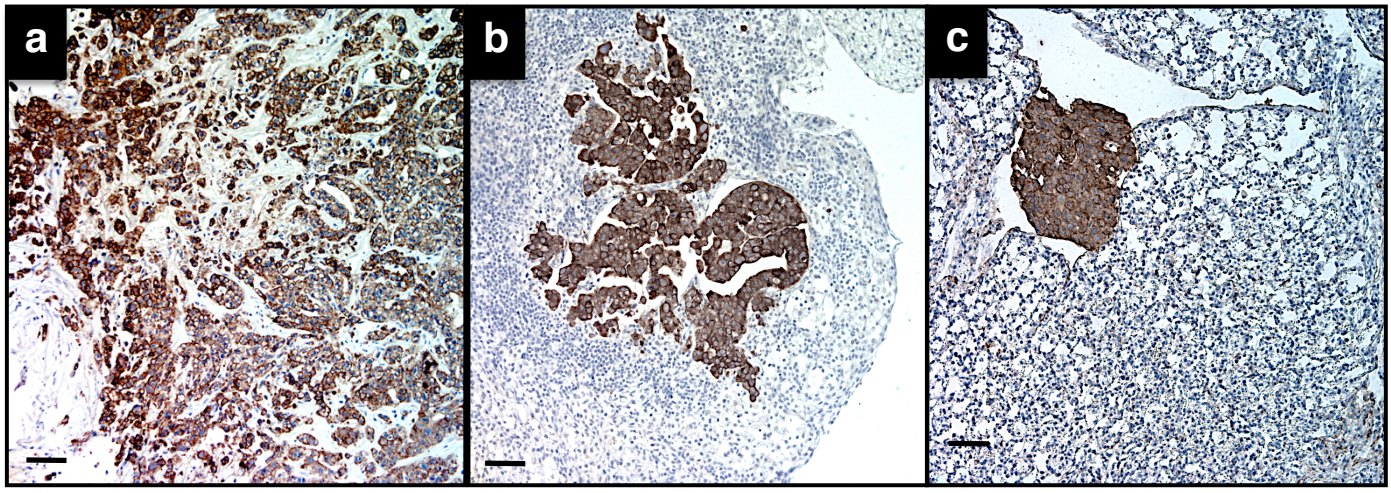

Supplementary Figure 17. Summary of metastasis from HCI-005. Top: Table illustrating the frequency of metastasis from three different tumors from three different generations of grafts, as well as clinical information on the patient from which HCI-005 was derived. Metastases were detected in lymph nodes of 5/13 (38%) of all mice examined, and in lungs of 8/13 (62%) of all mice examined. Bone metastasis was not evident in three bone samples examined (only samples with suspicious X-rays were examined histologically); however, bone metastasis was detected in the related line HCI-007 (see Supplementary Figure 18). Bottom: Representative images illustrating the histological characteristics of HCI-005 tumor graft (a) and lung metastases (b,c). All images in a-c show immunohistochemical staining for cytokeratin. Scale bars represent 100 microns.

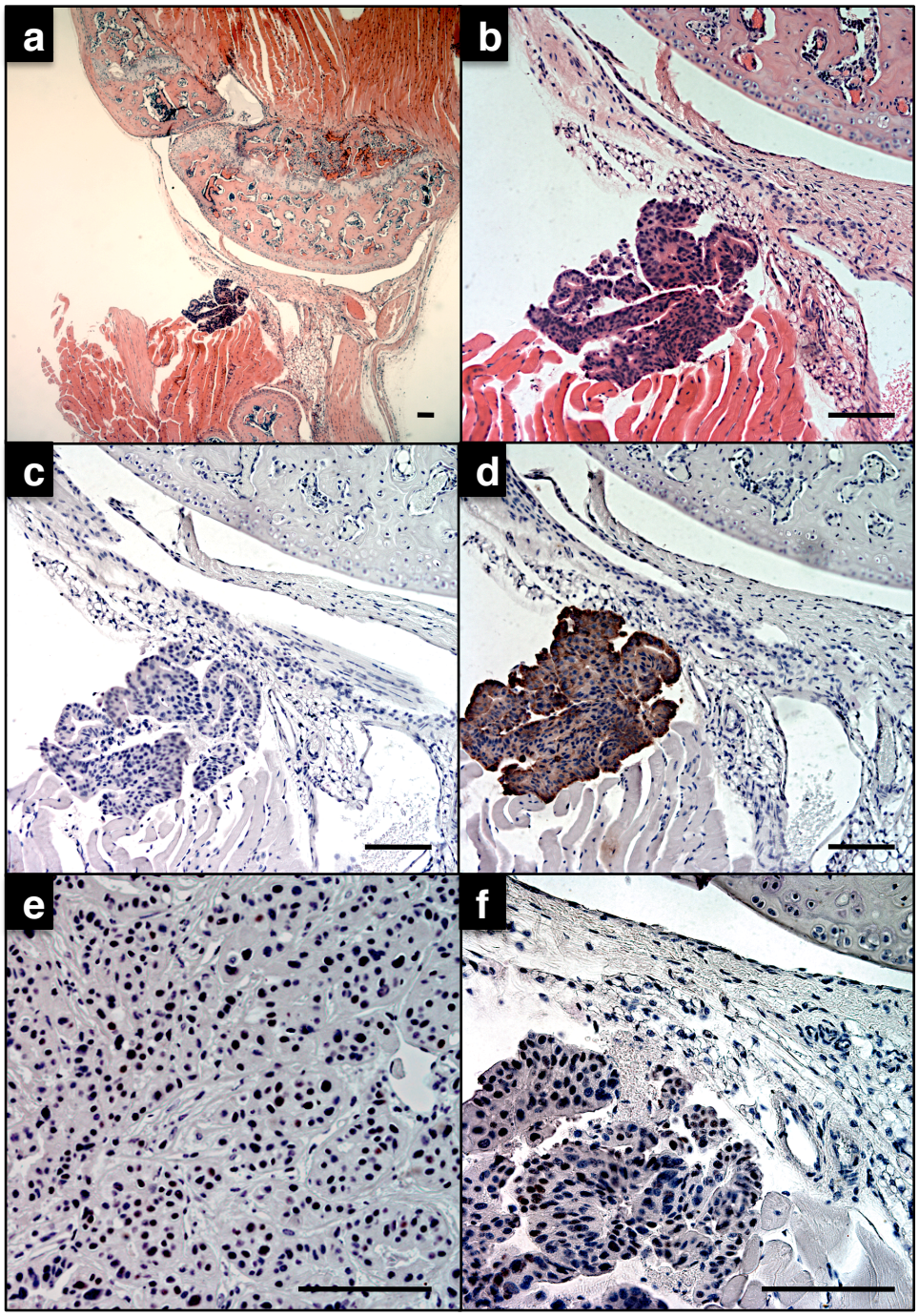

Supplementary Figure 18. Histology of ER+ bone metastasis from line HCI-007. Hind limbs from two mice carrying HCI-007 were examined histologically after evidence of bone loss was noted on X-ray analysis. a. H&E stain of the lesion, showing a tumor mass embedded between the muscle and bone. The lesion is located around the knee joint. b. Higher magnification of the lesion (H&E stained). c. Negative control for immunohistochemistry, showing no reactivity when only the secondary antibody was used. d. Immunohistochemistry revealed the metastastic lesion is positive for cytokeratin. e-f. Immunohistochemistry for ER on the primary tumor (e) and bone metastasis (f) of the same mouse.

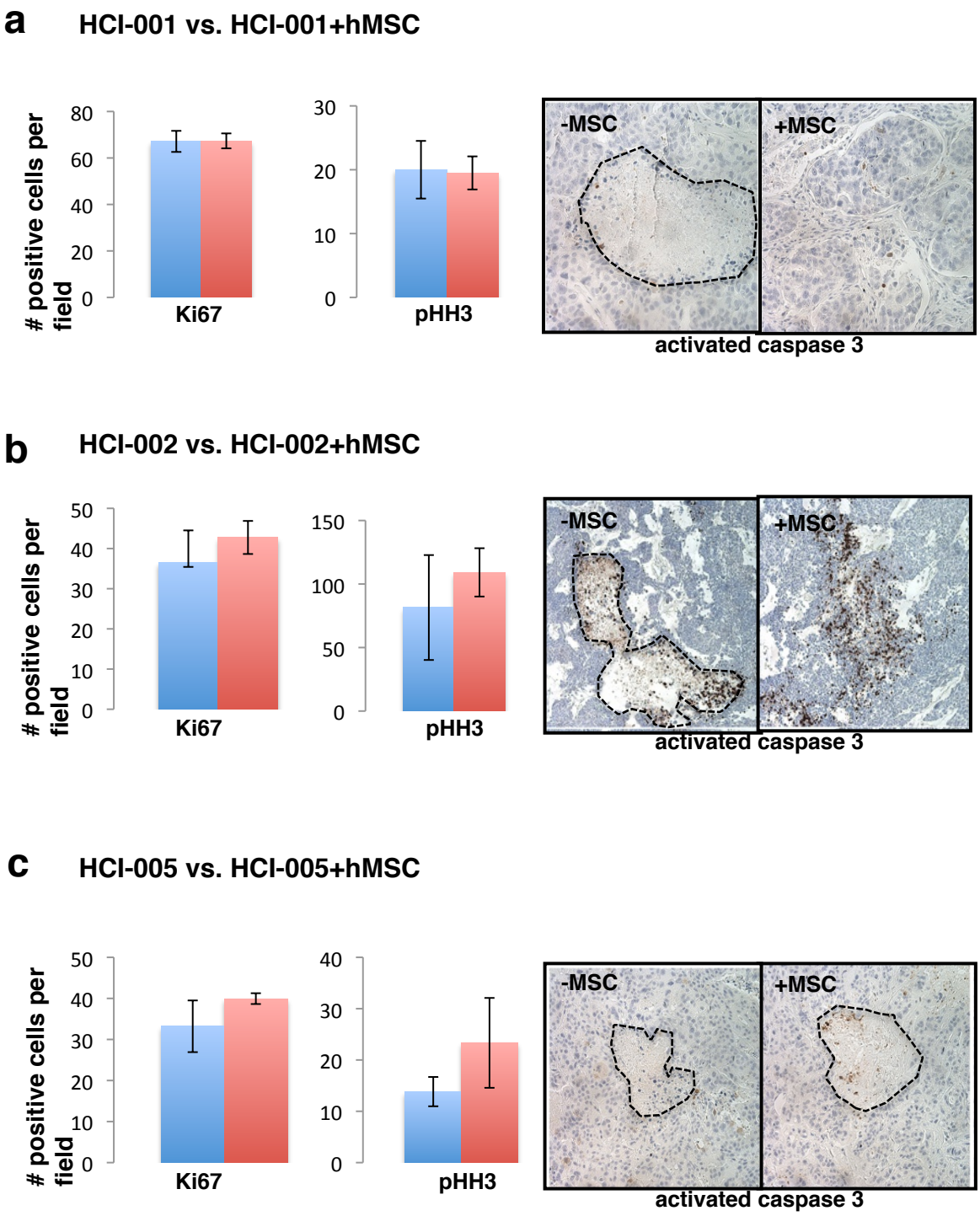

Supplementary Figure 19. Co-engraftment of hMSCs did not significantly affect tumor graft proliferation or apoptosis. a-c. Quantification of tumor cell proliferation or apoptosis, as determined by staining with antibodies specific for Ki67 (left) phosphorylated histone H3 protein (middle), and activated caspase 3 (right) in three different tumor grafts growing without hMSCs (blue bars) or with hMSCs (red bars). Data are represented as the average number of positive cells per field. Averages were calculated from 11-13 different fields per tumor, with at least 2 tumors per group. Areas of necrosis are highlighted with dotted lines in the images on the right.

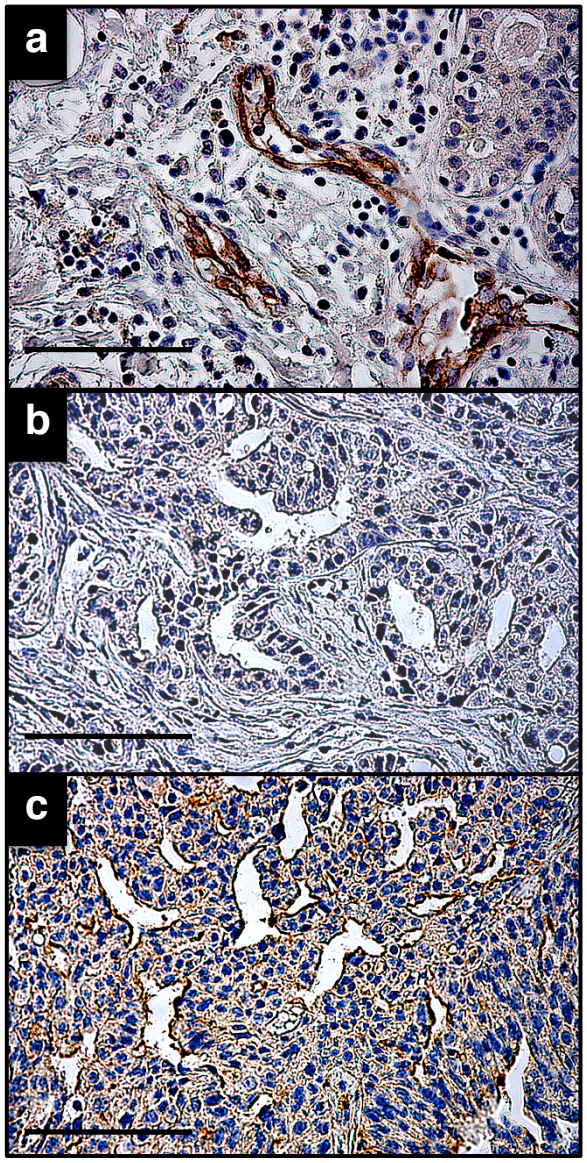

Supplementary Figure 20. hMSCs recruit mouse-derived endothelial cells to form a vascular network. Antibodies specific for human CD31 stain blood vessels in a representative patient specimen (a) but not in tumor grafts (b). On the other hand, antibodies specific for mouse or human CD31 stain the vasculature in tumor grafts (c).

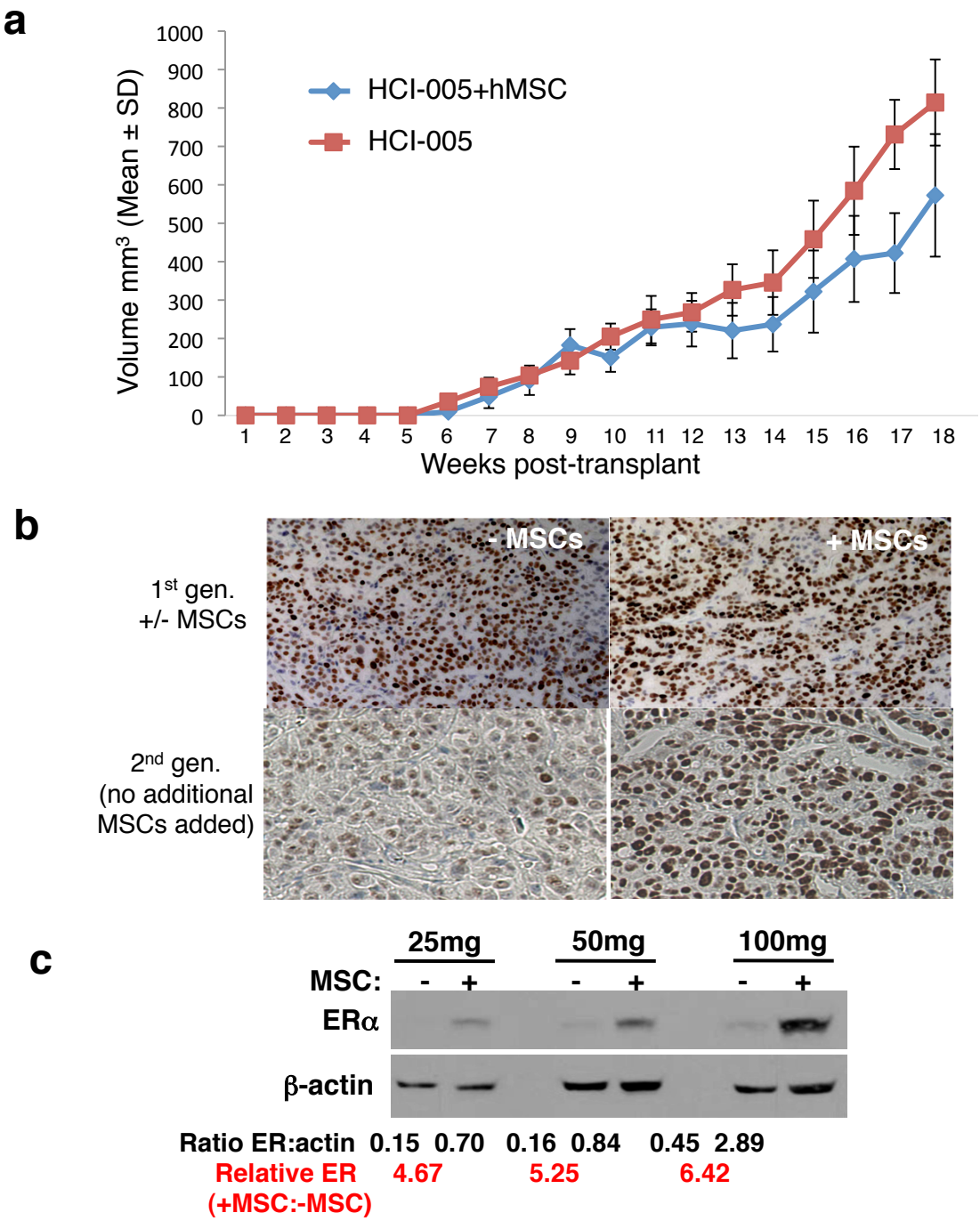

Supplementary Figure 21. Co-engraftment of hMSCs did not affect long-term tumor growth but promoted retention of ER expression. a. Growth rates are shown for next-generation HCI-005 grafts (without additional hMSCs), from tumors that were grown in the absence (red line) or presence (blue line) of hMSCs in the previous generation. b. Immunostaining for ER on tumorgrafts grown in the absence of hMSCs (top left image) or in the presence of hMSCs (top right image), compared to the next generation of tumors, which were re-transplanted without hMSCS. Stronger ER staining was observed in next-generation tumors from grafts that previously contained hMSCs (lower right image) versus next-generation tumors from grafts that previously had no hMSCs (lower left image). c. Representative semi-quantitative Western blot for ERα protein on next-generation HCI-005 tumor lysates grown without additional MSCs added. In the previous generation, the tumors were grown in the presence (+) or absence (-) of MSCs (shown at the top of the gel, along with the increasing amount of total protein loaded). The blot was re-probed with antibodies specific for β−actin as a loading control. Densitometry was used to quantify the relative levels of ERα to β-actin (shown in black below the gels). The relative levels of ER in tumors with or without MSCs, calculated on each dilution of protein, is shown at the bottom in red.